Radical-Driven Dissociation of Odd-Electron Peptide Radical Ions Produced in 157 nm Photodissociation

Liangyi Zhang and James P. Reilly
Department of Chemistry, Indiana University, Bloomington, Indiana, USA

Odd-electron $a + 1$ radical ions generated in the 157 nm photodissociation of peptide ions were investigated in an ion trap mass spectrometer. To localize the radical, peptide backbone amide hydrogens were replaced with deuterium. When the resulting radical ions underwent hydrogen elimination, no H/D scrambling was obvious, suggesting that without collisional activation, the radical resides on the terminal α-carbon. Upon collisional excitation, odd-electron radical ions dissociate through two favored pathways: the production of a-type ions at aromatic amino acids via homolytic cleavage of backbone C_α–C(O) bonds and side-chain losses at nonaromatic amino acids. When aromatic residues are not present, nonaromatic residues can also lead to a-type ions. In addition to a-type ions, serine and threonine yield c_{n-1} and $a_{n-1} + 1$ ions where n denotes the position of the serine or threonine. All of these fragments appear to be directed by the radical and they strongly depend on the amino acid side-chain structure. In addition, thermal fragments are also occasionally observed following cleavage of labile Xxx-Pro bonds and their formation appears to be kinetically competitive with radical migration. (J Am Soc Mass Spectrom 2009, 20, 1378–1390) © 2009 Published by Elsevier Inc. on behalf of American Society for Mass Spectrometry

Radicals derived from biological molecules are of considerable research interest since they can cause both beneficial and deleterious effects on living organisms [1–3]. Protein radicals undergo numerous radical-directed reactions, including backbone cleavages, disulfide cleavages, and side-chain losses [4–6]. These reactions show high complexity, low activation barriers, and poor selectivity due to the high reactivity of the radical and the small energy differences among reaction channels [7–9]. Most information about biological radicals has been derived from solution-phase reactions. With the advancement of mass spectrometry, much attention has been devoted to gas-phase biomolecular radicals since protein solution-phase structures can be preserved when they are introduced to a mass spectrometer using electrospray ionization (ESI) [10]. As a result, the gas-phase molecular reactivity may help to elucidate their reactivity under physiological conditions.

Many techniques and reactions have been developed to generate biomolecular radicals in the gas phase, including ion–ion (electron) interactions [11, 12], dissociation of peptide–metal complexes [13–16], and chemical modification with peroxycarbamate, azo, iodo, and nitroso functional groups along with ultraviolet (UV) photolysis of iodo-tyrosine [17–20]. Gas-phase reactions of multiply-charged protein and polypeptide ions with electrons or negatively-charged organic ions (electron capture dissociation, ECD or electron-transfer dissociation, ETD, respectively) yield abundant protein radical ions without changing protein conformation [11, 12, 21]. Although the majority of these hydrogen-rich radical ions readily dissociate, charge-reduced radical ions have also been abundantly observed [22, 23]. Peptides coordinated with copper (II)–amine complexes also give rise to strong peptide radical ions upon collisional activation as first reported by Siu and coworkers [13]. In fact, production of radical ions is not limited to copper (II) complexes. For example, O'Hair and coworker have shown that radical ions can be produced from salen complexes of various trivalent metal including chromium, manganese, iron, and cobalt [24]. It has been demonstrated that metal ions preferentially bind to the phenolic oxygen at tyrosine. Homolytic cleavage of metal–oxygen coordination bonds leads to tyrosyl radicals [13]. Deprotonated carboxylate can also bind to metal ions when peptides do not have tyrosine [14]. Peptide modification with functional groups including nitroso and peroxycarbonates also leads to abundant radical ions via homolytic cleavage of N–N or O–O bonds upon collisional activation [17–19]. Recently, Julian and coworkers have used UV photodissociation to generate protein or peptide radical ions [20, 25, 26]. After tyrosine is modified to iodo-tyrosine, photolysis of carbon–iodine bonds generates abundant carbon-centered radical ions.

Address reprint requests to Dr. J. P. Reilly, Department of Chemistry, Indiana University, 800 East Kirkwood Avenue, Bloomington, IN 47405, USA. E-mail: reilly@indiana.edu

1044-0305/09/$32.00
doi:10.1016/j.jasms.2009.03.026

Published online April 5, 2009
Received February 19, 2009
Revised March 30, 2009
Accepted March 31, 2009

Peptide ion fragmentation has been investigated experimentally and theoretically using various mass spectrometers [27–31]. Low-energy collision-induced dissociation (CID) of peptide ions yields primarily *y*- and *b*-type ions. This process can be well described by two types of fragmentation pathways: charge-induced and charge-remote dissociation. Charge-induced dissociation cleaves peptide backbone amide bonds that are weakened by a mobilized proton as described by the mobile proton model of Wysocki and coworkers [28]. Charge-remote dissociation cleaves the peptide backbone without involvement of a mobile proton. A typical example is the enhanced backbone fragmentation at aspartic acid and glutamic acid residues. Recently, fragmentation of peptide radical ions has been widely investigated. As pointed out by Laskin and coworkers, there are generally two types of radical ions: hydrogen-rich radical ions produced by ECD/ETD and hydrogen-deficient radical ions generated by a homolytic bond cleavage [16]. Fragmentation of these two types of radical ions leads to different product ions. Collisional dissociation of charge-reduced radical ions $[M + nH]^{(n-1)\bullet +}$ generated in ECD/ETD preferentially cleaves backbone N–C_α bonds, yielding a set of *c*- and $z^\bullet$-ions with high sequence coverage [22, 23]. A series of side-chain losses have also been observed [32–34]. This differs from collisional dissociation of even-electron peptide ions, which favors the formation of *b*- and *y*-type ions. The unusual fragmentation of charge-reduced radical ions has been attributed to radical-driven chemistry that can be described by a mobile hydrogen radical [35] or free radical reaction cascade [33, 36]. Theoretical studies have also shown that a radical is responsible for these unusual fragmentation processes [9]. Different from hydrogen-rich peptide radicals, hydrogen-deficient radical ions generated from peptide–metal complexes yield abundant *a*-type ions along with several side-chain losses [13, 16]. A similar dissociation pattern has also been observed for radical ions generated from peptides modified with a peroxycarbonated and nitroso functional group [17, 19]. To explain these results, the radical is believed to be mobilized upon activation and it then moves the internal amino acid side chains to induce fragmentation [16, 19]. Collisional dissociation of the photo-induced radical ions also leads to abundant *a*-type ions along with side-chain losses [20]. Hydrogen-deficient $z^\bullet$ radical ions generated in ETD have also been investigated by McLuckey and coworkers [37]. Upon collisional activation, abundant backbone fragments along with side-chain losses are observed, which is completely different from CID of even-electron peptide ions. Characteristic side-chain losses enable the identification of residues in a peptide.

One hundred fifty-seven nm photodissociation of singly-charged peptide ions with an N-terminal arginine yields abundant $a + 1$ radical ions as a result of homolytic cleavage of backbone C_α–C(O) bonds [38–40]. Although the majority of these radical ions undergo secondary fragmentation and generate even-electron *a*- and *d*-type ions, abundant $a + 1$ radical ions have still been observed in an ion trap mass spectrometer [39]. In this work, these odd-electron $a + 1$ radical ions were systematically investigated. The radical site was first probed by observing secondary hydrogen-elimination products. Radical ions were then isolated and fragmented by low-energy CID. Various observed backbone fragments and side-chain losses are discussed. Observation of radical ion fragmentation provides insights about radical migration in the gas phase.

Experimental

Materials

Peptides RYLGYLE and RPPGFSP were purchased from Sigma (St. Louis, MO). All other peptides were synthesized in-house or by Sigma Genosys (The Woodlands, TX). Deuterium oxide (D_2O) was supplied by Cambridge Isotope Laboratories, Inc. (Andover, MA). Acetonitrile (ACN) was purchased from EMD Chemicals, Inc. (Gibbstown, NJ). Formic acid was obtained from Fluka Chemika GmbH (Buchs, Switzerland). Acetic acid was also obtained from Fluka Chemika GmbH.

Peptide H/D Exchange Reaction

Peptide deuterium-labeling was performed using an H/D exchange reaction as previously described [39]. In brief, peptide stock solutions were dried with a Speed Vac and then resuspended into a deuterated acidic solvent containing 49.95% D_2O, 49.95% CAN, and 0.10% formic acid. Each solution was incubated at room temperature for 30 min. To avoid the moisture in the air, all solutions were made in a glove bag filled with dry nitrogen. Before the mass spectrometric analysis, the sample inlet line was flushed with D_2O for 20 min. During electrospray, the ESI-source chamber was purged with dry nitrogen to avoid H/D back exchange with the moisture in the air.

Mass Spectrometry

An LTQ linear ion trap mass spectrometer (Thermo Fisher, San Jose, CA) was used for mass spectrometric analysis in this work. Photodissociation in the LTQ was set up as previously described [39, 41]. Briefly, an F_2 laser (EX100HF-60; GAM laser, Orlando, FL) was introduced axially into the trap from its back side. The 157 nm vacuum ultraviolet (VUV) laser was triggered by LTQ activation pulses, producing 3 mJ of light in a 10 ns pulse. After aperturing, only about 40 uJ of light actually entered the ion trap to dissociate the peptide ions. All the product ions were scanned out to the LTQ duel detectors or isolated for further fragmentation as normal instrument operating modes. In this work, only the monoisotopic component of the peptide ion signal was photodissociated to yield radical ions. Subsequently,

odd-electron $a + 1$ radical ions were isolated and then subjected to CID.

All peptides were prepared in 2 uM solutions with a solvent containing 49.5% H_2O, 49.5% CAN, and 1.0% acetic acid. Each peptide solution was directly infused into the ESI source of the LTQ with a syringe pump at a flow rate of 3 uL/min.

Results and Discussion

Previously we have demonstrated that 157 nm photodissociation of singly-charged peptide ions yields abundant $a + 1$ radical ions [38, 39]. In the present work, these odd-electron radical ions were isolated in an ion trap mass spectrometer to study their structure and fragmentation behavior.

Radical Site

Each photolytically-generated radical is assumed to be initially located on the terminal α-carbon. It is of interest to investigate whether the unpaired electron transfers to other sites. $a + 1$ radical ions usually undergo β-elimination to form a-type ions. At most amino acids, they can lose a backbone amide-hydrogen or side-chain β-hydrogen, yielding a-type ions with a $N{=}C_\alpha$ bond on the peptide backbone or a $C_\alpha{=}C_\beta$ bond at the side chain [39]. Two exceptions are glycine and proline, which have no β- and amide-hydrogens, respectively. Therefore, the radical site can be revealed by observing a-type ion formation in radical ions terminated by these residues (Scheme **1**). If the radical transfers to other residues, both hydrogen elimination pathways would be expected. To differentiate the two pathways, backbone amide hydrogens were replaced with deuterium by H/D exchange as previously described [39]. Two peptides RGGQGG and RAAADPAAA were used to generate radical ions terminated with glycine and proline. Formation of a-type ions from these two radical ions was then investigated.

Figure 1a and b show the expanded views of the $a_5 + 1$ peak ($[RGGQG]^{+\bullet}$) in the photodissociation spectra of hydrogenated and deuterated peptide RGGQGG, respectively. It is evident that radical ions are abundant in both spectra, suggesting that these odd-electron radical ions are stable in an ion trap mass spectrometer. As demonstrated previously, formation of a-type ions in 157 nm peptide photodissociation proceeds via hydrogen loss from $a + 1$ radical ions [39]. In the hydrogenated spectrum, an a_5 ion is formed by losing a hydrogen from the radical ion. However, in the deuterated spectrum, only deuterium-loss product is abundant; the hydrogen-loss peak is at the level of noise. This indicates that the radical resides at the terminal glycine. If the radical transferred to the glutamine side chain, a hydrogen loss should also have been detected in Figure 1b (as shown in Scheme **1a**). Figure 1c and d display the expanded views of the $a_6 + 1$ peak ($[RAAADP]^{+\bullet}$) in the photodissociation spectra of hydrogenated and deuterated peptide RAAADPAAA, respectively. Similar to Figure 1a, photodissociation of the hydrogenated form yields both the radical ion and a-type ion corresponding to hydrogen loss. However, strikingly different from Figure 1b, the deuterated radical ion undergoes primarily a hydrogen-elimination reaction. The deuterium-loss peak is at the level of noise. This indicates that the radical is located on the terminal proline since proline has only side-chain β-hydrogen for elimination. If the radical transferred to another amino acid side-chain, loss of a deuteron would also have been observed in Figure 1d (as shown in Scheme **1b**).

The above two examples demonstrate that the unpaired electron in the $a + 1$ radical ions remains on the terminal α-carbon and does not transfer to other amino acids when the ion is not collisionally activated. This indicates that $a + 1$ radical ions are fairly stable in the ion trap mass spectrometer [42]. Therefore, 157 nm photodissociation of peptide ions can be used to generate odd-electron radical ions. Because the radical site is known, these photo-induced radical ions can provide information about radical migration caused by collisional activation.

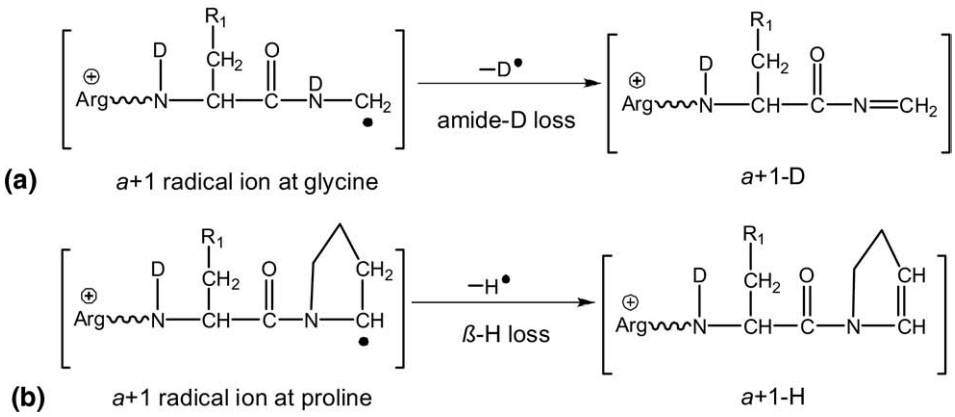

Scheme 1

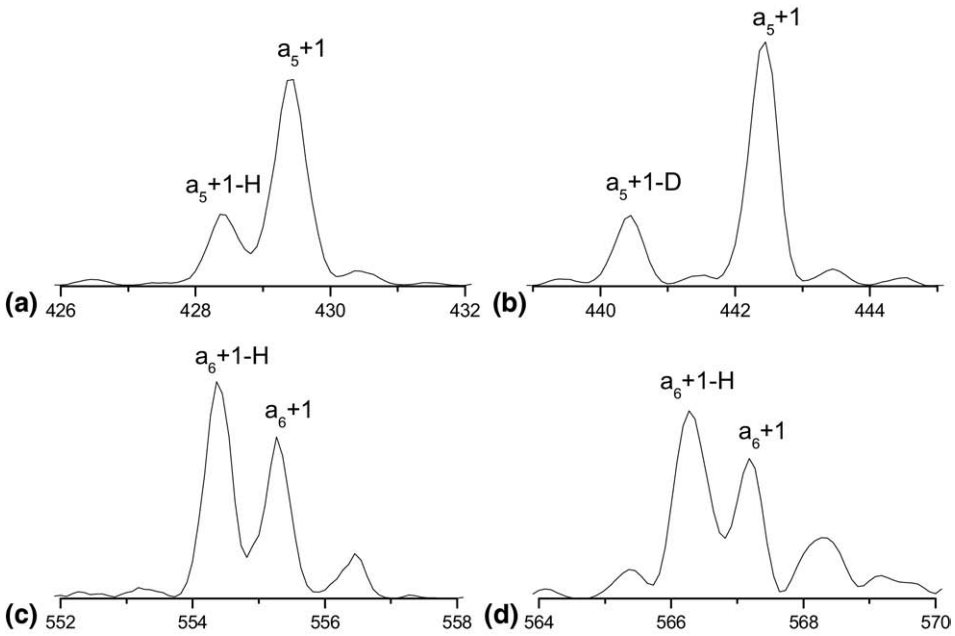

Figure 1. Expanded views of a_5 + 1 ions in the photodissociation spectrum of (**a**) hydrogenated, (**b**) deuterated peptide RGGQGG, and a_6 + 1 ions in the photodissociation spectrum of (**c**) hydrogenated and (**d**) deuterated peptide RAAADPAAA.

Collisional Dissociation of Radical Ions

In the ion trap mass spectrometer, various photo-induced a + 1 radical ions were isolated and then collisionally dissociated. Figure 2a displays the CID spectrum of a_8 + 1([RFSWGAEG]$^{+\bullet}$) ions from RFSWGAEGQ. It is dominated by a series of a-type ions (a_2, a_3, and a_4) as well as three neutral losses of 17, 30, and 72 Da. The a_2 and a_4 ion are abundant and they correspond to backbone C_α–C(O) bond cleavage at aromatic residues phenylalanine and tryptophan, respectively. The a_3 ion is also formed although it is much less abundant than the other two. Observation of a-type ions is consistent with previous experiments on radical ion fragmentation [13, 16, 20]. Loss of 17 Da is mainly attributed to release of hydroxyl radical since it is abundantly observed primarily for radical ions with serine or threonine. Loss of 30 Da corresponds to removal of formaldehyde from serine side chain. Both serine side-chain losses have also been previously observed [34, 37]. Loss of 72 Da corresponds to removal of even-electron acrylic acid from glutamic side chain. In addition, a small c_2 ion is also formed following cleavage at the N-terminal side of serine. For comparison, the even-electron a_8 ion was also collisionally dissociated and the results are displayed in Figure 2b. The asterisk denotes loss of ammonia. The spectrum is dominated by loss of ammonia along with b_7 ions. All of these fragments are typical thermal fragments [29, 31]. It is evident that radical ions yield completely different fragments as their even-electron counterparts. The unusual fragmentation of odd-electron ions implies that the radical plays an important role in the dissociation process [13, 14, 16, 25, 43–45].

a_7 + 1 and a_6 + 1 ions from the same peptide were also collisionally dissociated and the results are displayed in Figure 2c and d. Both spectra appear very similar to Figure 2a. Fragment ions terminated by aromatic residues phenylalanine and tryptophan, a_2 and a_4, are again abundant. Both a_3 and c_2 are also observed at serine. The only difference occurs in Figure 2d where loss of 72 Da is missing because the a_6 + 1 ion does not contain glutamic acid. Even though the radical in the three a + 1 ions is initially located at different amino acids, it eventually transfers to the same residues and induces similar fragmentation processes.

To explain the production of a-type ions and side-chain losses in the above examples, we assume that the radical moves from the C-terminal α-carbon to the internal amino acids regardless of its initial location. This is consistent with the high radical mobility indicated by theoretical and experimental observations [26, 46]. As shown in Scheme **2**, after the radical moves to the side-chain β-carbon via hydrogen abstraction, it facilitates the cleavage of backbone C_α–C(O) bonds, forming an even-electron a-type ion after loss of an odd-electron carbonyl radical. This pathway is consistent with previous experiments on radical ion dissociation [13, 16, 19, 20].

Formation of a*-Type Ions*

Since a-type ions terminated by phenylalanine and tryptophan are consistently abundant in the above three examples, we hypothesize that aromatic amino acids favor a-type ion formation because they can stabilize β-radicals through conjugation with the aromatic ring

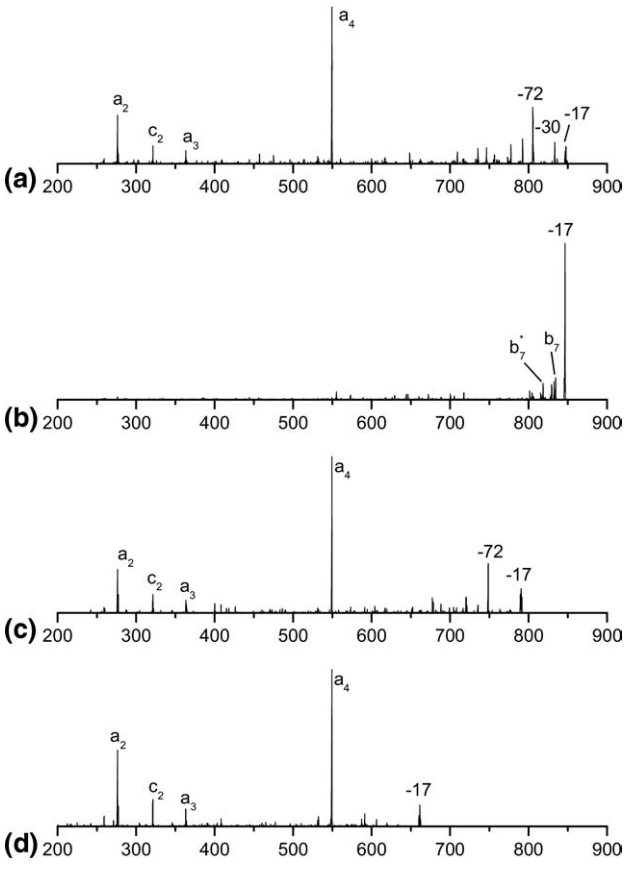

Figure 2. CID spectra of (**a**) a_8 + 1, (**b**) a_8, (**c**) a_7 + 1, and (**d**) a_6 + 1 ions from peptide RFSWGAEGQ. In all figures, asterisk denotes loss of an ammonia.

(Scheme 2). To test this hypothesis, a series of a + 1 radical ions from peptide RYLGYLE were fragmented and the results are displayed in Figure 3. The CID spectrum of the a_6 + 1 ion is displayed in Figure 3a. It is dominated by a_2 and a_5 ions terminated by tyrosine residues along with three neutral losses. It is evident that tyrosine also favors formation of a-type ions. The neutral losses of 56 and 43 Da correspond to losses of 2-methylpropene and 2-propyl radical, respectively. These are both associated with leucine side-chain fragmentation as reported in previous ECD experiments [25, 34, 47]. The loss of 106 Da corresponds to removal of a p-quinomethide (H_2C=⟨⟩=O) that has also been observed previously [43, 48]. All of these side-chain losses will be discussed in the following section. Figure 3b displays the CID spectrum of a_5 + 1 ions. It is essentially identical to Figure 3a except that a_5 ions are not observed. Figure 3c displays the CID spectrum of a_3 + 1 ions. Dominant a_2 ions are also observed. The above examples demonstrate the enhanced production of a-type ions terminated by aromatic amino acids. This is consistent with the pathway in Scheme 2 since the reactive intermediate β-radicals can be stabilized by the conjugational effect of the aromatic ring. It is noteworthy that all of the above three a+1 ions yield abundant a_2 ions even though the radical is initially located at different residues. This indicates that the radical ion fragmentation is less strongly influenced by the initial radical location than by the amino acid side chain.

In addition to the abundant a-type ions formed at aromatic amino acids, an a_3 ion terminated by nonaromatic residue serine also appears in Figure 2a, c, and d. This can also be explained by the pathway in Scheme 2 since the β-radical at serine is stabilized by the β-hydroxyl group. Nevertheless, the intensity of this a-type ion is much lower than those terminated by aromatic residues.

To further investigate a-type ion formation, several radical ions that did not contain aromatic amino acids were collisionally dissociated and the results are displayed in Figure 4. The CID spectrum of $[RAAALA]^{+\bullet}$ (Figure 4a) is dominated by an a_5 ion and two neutral losses corresponding to leucine side-chain fragmentation. The a_5 ion is terminated by a nonaromatic residue leucine. This is drastically different from Figure 3 in which a-type ions are not formed at leucine from radical ions that contain aromatic amino acids. Likewise, the CID spectrum of radical ion $[RAAAIA]^{+\bullet}$ (Figure 4b) is also dominated by an a_5 ion formed at isoleucine. The neutral losses of 56 and 29 Da correspond to isoleucine side-chain fragmentations that are discussed in the following section. a_4 ions are also formed when the radical ion $[RAAQA]^{+\bullet}$ is collisionally dissociated (Figure 4c). The neutral losses of 71 and 58 Da are associated with glutamine side-chain fragmentation. In contrast, collisional dissociation of $[RGGMG]^{+\bullet}$ does not yield a-type ions (Figure 4d). Instead, the spectrum is dominated by four neutral losses of 15, 47, 61, and 74 Da that correspond to release of $CH_3\bullet$, $CH_3S\bullet$, $CH_3SCH_2\bullet$, and $CH_3SCH{=}CH_2$, respectively.

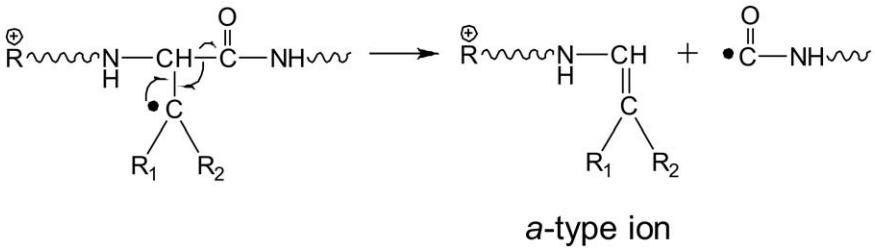

Scheme 2

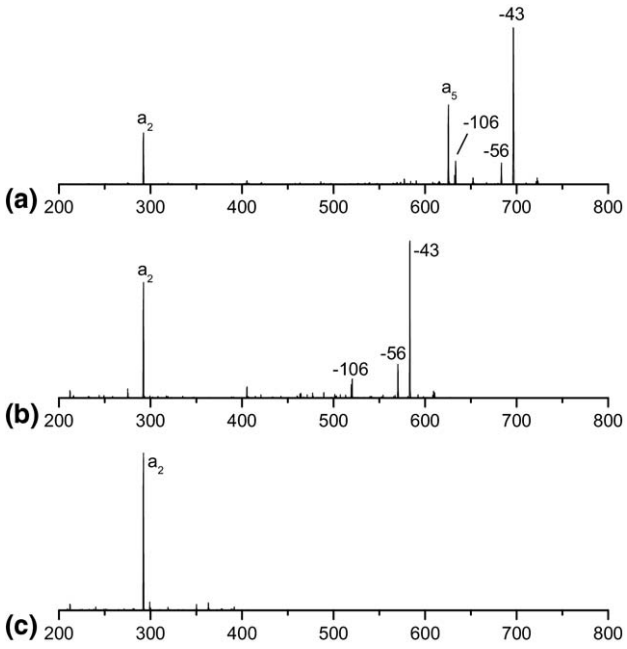

Figure 3. CID spectra of (**a**) a_6 + 1, (**b**) a_5 + 1, and (**c**) a_3 + 1 radical ions from peptide RYLGYLE.

a-Type ions have been observed at most nonaromatic amino acids when radical ions do not contain aromatic residues. This is presumably because the β-carbon at these nonaromatic residues becomes the preferred radical site when there is no more energetically favorable site in the sequence. This is consistent with Julian and coworkers' results that the bond dissociation energy of C_β-H mediates the backbone fragmentation of radical ions [25]. Methionine is an exception because in addition to forming *a*-type ions, the methionine β-radical can also undergo a competitive β-elimination pathway by loss of a $CH_3S\bullet$ radical. Since $CH_3S\bullet$ is a better leaving group than the carbonyl radical during *a*-type ion formation, loss of $CH_3S\bullet$ (47 Da) is more energetically favorable than formation of *a*-type ions. In addition, based on the Scheme **2** mechanism, glycine cannot form *a*-type ions since it does not contain a β-carbon. *a*-Type ions terminated by alanine are also not formed because in this case the β-radical is primary and less stable.

Side Chain Losses

As shown in the above examples, abundant side-chain losses from various nonaromatic residues are observed. These losses depend on amino acid side-chain structure. For example, leucine and isoleucine lead to different neutral losses (Figure 4a and b) although they are isobaric. At most nonaromatic residues, two types of side-chain losses occur: loss of the whole side chain and loss of a β-substitute. These side-chain losses are radical-driven since they are not formed during fragmentation of their even-electron forms. It has been demonstrated that a radical can induce a number of side-chain losses via different radical intermediates [19, 20, 25, 32, 47]. The two observed types of side-chain losses from leucine can be well explained by α- and γ- radical intermediates as shown in Scheme **3**. In Scheme **3a**, the radical is located at the α-carbon and it facilitates homolytic cleavage of the side-chain C_β–C_γ bond, forming an even-electron fragment after releasing an odd-electron β-substitute. In Scheme **3b**, the radical is located at the γ-carbon and it leads to homolytic cleavage of the side-chain C_α–C_β bond, forming an odd-electron radical ion after leaving the whole side chain as an even-electron species. It is evident in Scheme **3** that leucine and isoleucine lead to different side-chain losses because of their different side-chain structure. This is consistent with previous results on radical ion fragmentation [47].

Methionine undergoes more extensive side-chain fragmentation than most other nonaromatic amino acids. As shown in Figure 4d, side-chain losses of 15, 47, 61, and 74 Da can be attributed to methionine. As noticed previously, they correspond to removal of $CH_3\bullet$, $CH_3S\bullet$, $CH_3SCH_2\bullet$, and $CH_3SCH{=}CH_2$, respectively. Proposed reaction pathways are displayed in Scheme S1. The first two pathways are similar to Scheme **3** in which the α-radical leads to removal of the whole side-chain $CH_3SCH = CH_2$ (Scheme S1-A) and the γ-radical eliminates the β-substitute $CH_3SCH_2\bullet$

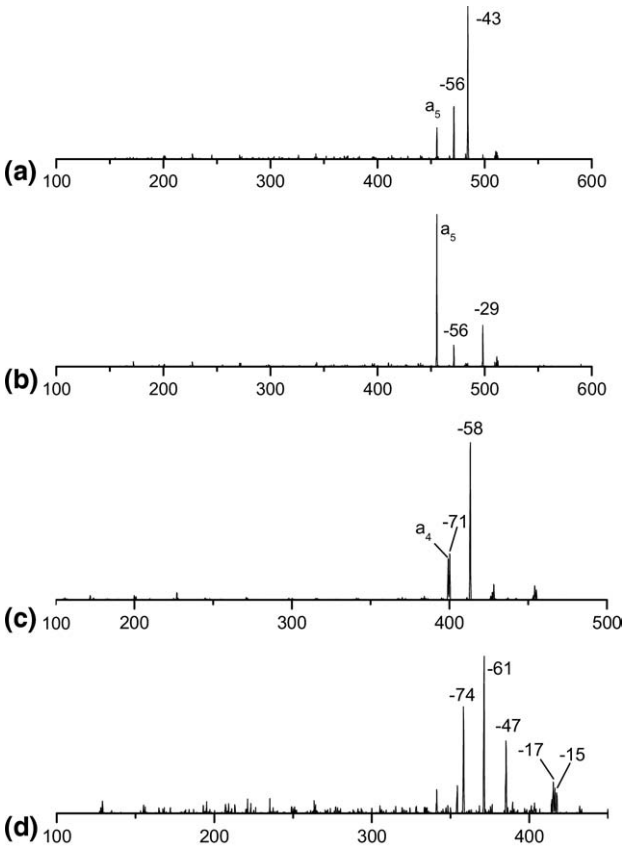

Figure 4. CID spectra of (**a**) $[RAAALA]^{+\bullet}$, (**b**) $[RAAAIA]^{+\bullet}$, (**c**) $[RAAQA]^{+\bullet}$, and (**d**) $[RGGMG]^{+\bullet}$.

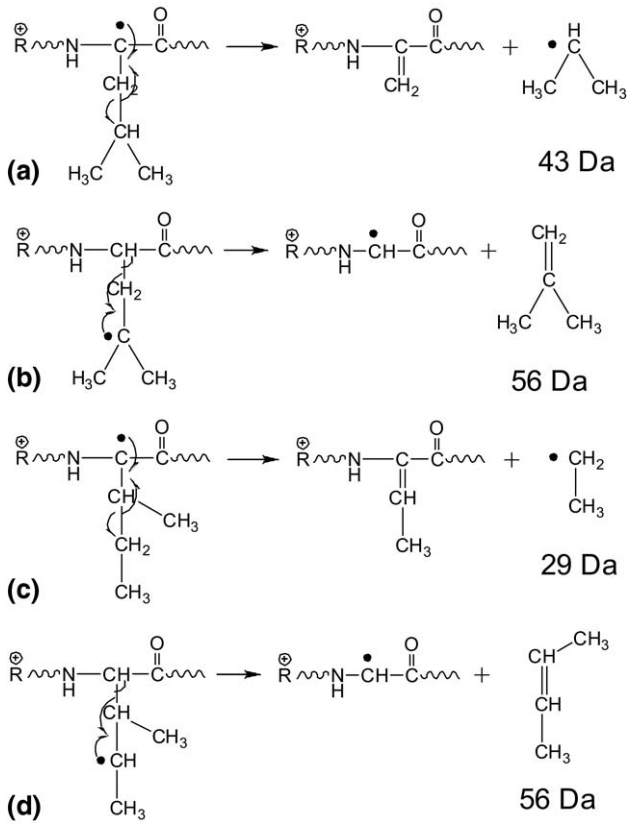

Scheme 3

(Scheme S1-B). Although the γ-radical can also lead to removal of the δ-substitute CH_3• (Scheme S1-C), this pathway is disfavored since the methyl radical is not a good leaving group. As discussed previously, the β-radical at methionine prefers to release CH_3S• (Scheme S1-D) instead of forming *a*-type ions. In summary, all C–C and C–S bonds on the methionine side chain can be dissociated by radical-driven processes.

Side-chain losses from various amino acids during radical ion fragmentation have been observed and are summarized in Table 1. Most nonaromatic amino acids tend to lose both the whole side-chain and some part of it as described by Scheme **3a** and **b**. Except for tyrosine, this is not observed at aromatic amino acids. This is reasonable since both side-chain fragmentation pathways are thermodynamically disfavored at aromatic amino acids. Loss of the β-substituent (analogous to Scheme **3a**) is disfavored because the C_β–C_γ bond is difficult to break due to conjugation with the aromatic ring; loss of the whole side-chain (Scheme **3b**) does not occur since the γ-radical is not formed at aromatic amino acids. Uniquely, tyrosine loses *p*-quinomethide (106 Da) via a pathway in which a phenol oxygen-radical undergoes radical rearrangement, leading to homolytic cleavage of the C_α–C_β bond [13]. Proline does not yield side-chain losses because its side-chain is cyclic. Glycine does not have a β-carbon. Although alanine has a methyl side-chain, it cannot lose the methyl since cleavage of the C_α–C_β bond requires a γ-carbon. These observations are consistent with previous results on radical ion fragmentation [15, 25, 34, 47].

Side-chain losses occur at two-thirds of amino acids. They are easily identified and thus can provide important peptide sequencing information. For example, the side-chain losses in the radical ion fragmentation can distinguish isobaric leucine and isoleucine [25, 34, 47]. This is significant because these two residues represent 16.7% of all amino acids in nature and they are not

Table 1. Loss of odd-electron and even-electron species from amino acid side chains in fragmentation of *a* + 1 radical ions[a]

Amino acids	Odd-electron losses (Da)	Assignment	Even-electron losses (Da)	Assignment
Glycine (G)	—	—	—	—
Alanine (A)	—	—	—	—
Proline (P)	—	—	—	—
Leucine (L)	43	$(CH_3)_2CH$·	56	$(CH_3)_2C{=}CH_2$
Isoleucine (I)	29	CH_3CH_2·	56	$CH_3CH{=}CHCH_3$
Methionine(M)	15	CH_3·	74	$CH_3SCH{=}CH_2$
	47	CH_3S·		
	61	CH_3SCH_2·		
Asparagine (N)	44	H_2NCO·	—	—
Glutamine (Q)	58	H_2NCOCH_2·	71	$H_2NCOCH{=}CH_2$
Aspartic acid (D)	—	—	44	CO_2
Glutamic acid (E)	—	—	72	$HOOCCH{=}CH_2$
Serine (S)	17	·OH	30	$CH_2{=}O$
			18	H_2O
Threonine (T)	17	·OH	44	$CH_3CH{=}O$
			18	H_2O
Tyrosine (Y)	—	—	108	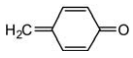
Phenylalanine (F)	—	—	—	—
Tryptophan (W)	—	—	—	—
Histidine (H)	—	—	—	—

[a]The mass of side chain losses is rounded to its nominal mass.

distinguished by low-energy peptide fragmentation [49]. Most side-chain losses are unique to amino acids, so their observation provides information about peptide composition. Identification of several amino acids in a peptide could be used to constrain database-searching results [25].

Competition Between Backbone Fragmentation and Side Chain Losses

Although *a*-type ions and side-chain losses are formed via similar radical-driven processes, they vary significantly in abundance. For example, in Figure 4a, at leucine, loss of 43 Da is the most abundant peak while the a_5 ion is the least abundant one. Interestingly, the peak distribution is different for the isobaric isoleucine residue as shown in Figure 4b. In this case, the a_5 ion is the most abundant peak. Similar peak distributions have been observed at all leucine and isoleucine residues. This indicates that the competition between backbone fragmentation and side-chain losses is strongly affected by the amino acid side-chain structure. In fact, the observed fragment abundances can be explained by the relative stabilities of their radical intermediates. For example, at leucine (Figure 4a), the a_5 ion is the least abundant peak because the secondary β-radical is much less stable than the tertiary α- and γ-radicals (Scheme **3a** and **b**). At isoleucine (Figure 4b), loss of 56 Da is the least abundant peak since the γ-radical is a secondary radical (Scheme **3d**). The a_5 ion is the most abundant peak because the β-radical is a tertiary radical. In Figure 4c, loss of 58 Da is the dominant peak since the α-radical is tertiary while the β- and γ-radicals are secondary. In Figure 4d, loss of the β-substituent (61 Da) is the most abundant peak because the α-radical is tertiary. Moreover, the stability of the β-radical also explains the preferential formation of *a*-type ions at aromatic amino acids.

It is evident that upon activation, an unpaired electron that is located on the C-terminal carbon of a fragment ion can transfer to the α-, β-, and γ-carbon of other amino acids, leading to a variety of smaller fragments. Competition among these fragmentation pathways is strongly affected by the relative stability of the radical intermediates. Relative radical stabilities have been predicted by theoretical calculations [50]. The most stable radicals include tertiary radicals and some secondary β-radicals at aromatic residues as well as serine and threonine. Only tertiary radicals can compete with the stability of secondary β-radicals at aromatic residues and so side-chain losses at nonaromatic residues and *a*-type ions terminated by aromatic residues are observed. For radical ions without aromatic residues, *a*-type fragments and side-chain losses corresponding to secondary radicals can also be observed. This is reasonable since radical-driven fragmentations proceed normally with low activation barriers [51]. As a result, the thermodynamics of different fragmentation channels determines the relative abundances of their products. This is also consistent with Julian and coworkers' results that C_β–H bond-dissociation energy (BDE) correlates well with the preferential backbone fragmentation along peptide backbone [25].

Radical-Driven Fragmentation at Serine and Threonine

As shown in Figure 2a, c, and d, a c_2 ion was observed N-terminal to serine. To test whether serine induced this unusual fragmentation, several serine- and threonine- containing radical ions were fragmented. Figure 5a displays the CID spectrum of a_6 + 1 ions ($[RSAASL]^{+\bullet}$) generated by photodissociation of peptide ion RSAASLNS. It is dominated by several *a*- and *c*-type ions as well as a few neutral losses in the high mass region. Associated with serine 2, a_2, c_1, and a_2-H_2O are observed. At serine 5, a_5, c_4, and a_4 + 1 are observed. The neutral losses of 43 and 56 Da correspond to leucine side-chain fragmentation while the 17 and 30 Da losses are associated with serine side-chain fragmentation. The neutral loss of 35 Da corresponds to the combined loss of ammonia and water. For comparison, the a_4 + 1 ions ($[RSAA]^{+\bullet}$) were also collisionally dissociated and the results are displayed in Figure 5b. Similar to Figure 5a, four backbone fragments a_2, a_2-H_2O, c_1, and a_1 + 1 are again formed. The neutral losses are similar to those in Figure 4a except that the 43 and 56 Da peaks are

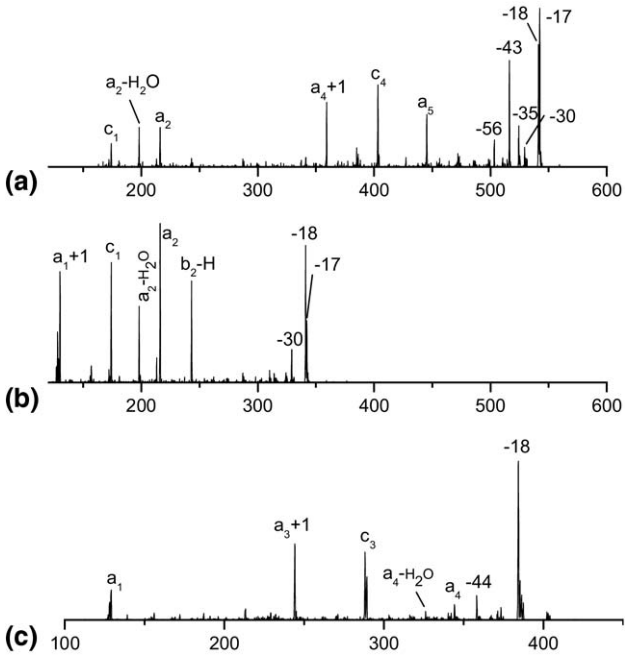

Figure 5. CID spectra of (**a**) a_6 + 1, (**b**) a_4 + 1 radical ions from peptide RSAASLNS, and (**c**) a_5 + 1 radical ions from peptide RGGTGG.

missing because the radical ion does not contain leucine. The b_2-H ion corresponds to abstraction of a hydrogen from the regular b_2 ion that is formed via a low-energy charge-directed dissociation channel [13, 14, 16, 43, 45, 52]. These hydrogen-deficient *b*-type ions have been observed in previous radical ion fragmentation experiments [13, 14, 16, 43, 45]. Their formation will be discussed in the following section. Threonine-containing radical ions were also collisionally dissociated. Figure 5c displays the CID spectrum of a_5 + 1 ions generated by photodissociation of peptide ion RGGTGG. It is evident that abundant a_4, c_3, and a_3 + 1 are formed suggesting threonine involvement. The a_4-H_2O ion is also formed although it is really low in abundance. Analogous to serine, the neutral loss of 18 Da corresponds to loss of water and neutral losses of 17 and 44 Da correspond to release of hydroxyl radical and acetaldehyde, respectively. In addition, an a_1 ion is also observed with low abundance. It is noteworthy that the c_3 + 1 ion is also observed in this case. However, c + 1 ions have not been observed in other examples, so it is not clear whether formation of the c_3 + 1 ion is associated with the serine/threonine residue.

These data indicate that serine and threonine induce unusual backbone fragmentation, yielding three backbone fragments: a_n, c_{n-1}, and a_{n-1} + 1 ions where n denotes the position of serine or threonine. In Figures 2a, c, and d, a_3, and c_2 ions are also evident. Expanded views of the a_2 peaks (Figure S1), which can be found in the electronic version of this article, show that a_2 + 1 are also formed. In general, odd-electron a+1 ions are not formed unless serine or threonine is present. For example from a study of peptide RFSWGAEGQ, Figure S1 shows that a_4 + 1 ions are not formed while abundant a_4 ions were observed at aromatic amino acid tryptophan. Formation of *a*-type ions at serine is similar to the general pathway in Scheme **2**. In this pathway, the β-radical induces homolytic cleavage of the adjacent C_α–C(O) bond, forming *a*-type ions by releasing a carbonyl radical. Since the enol structure is not stable, it probably isomerizes to the more stable aldehyde.

Besides forming *a*-type ions, β-radicals can, in principle, also lead to cleavage of the backbone N–C_α bond. This pathway is usually kinetically disfavored by several orders of magnitude as indicated by recent theoretical calculations [53]. However, our experimental results indicate that serine and threonine facilitate this process, leading to *c*-type ions. As shown in Scheme **4a**, the hydroxyl hydrogen can transfer to the amide-nitrogen, forming an even-electron *c*-type ion. Since they are unique to serine and threonine residues, *c*-type ions can be used to identify the presence of these amino acids during peptide sequencing.

Serine and threonine also lead to abundant water loss (M − H_2O) and a_n-H_2O fragments that are not formed at other amino acids as shown in Figure 5a–c. Both fragments should be formed via radical-driven processes since they do not appear in the CID spectrum of the even-electron *a*-type ions. The pathway for loss of water is hypothesized in Scheme **4b**. Through a five-member ring radical rearrangement, the α-radical at serine releases water, yielding a nitrogen-centered radical. This radical is not stable and it switches to the more stable β-radical. In addition to the isomerization process, the nitrogen-centered radical can also undergo two secondary β-elimination pathways as shown in Scheme

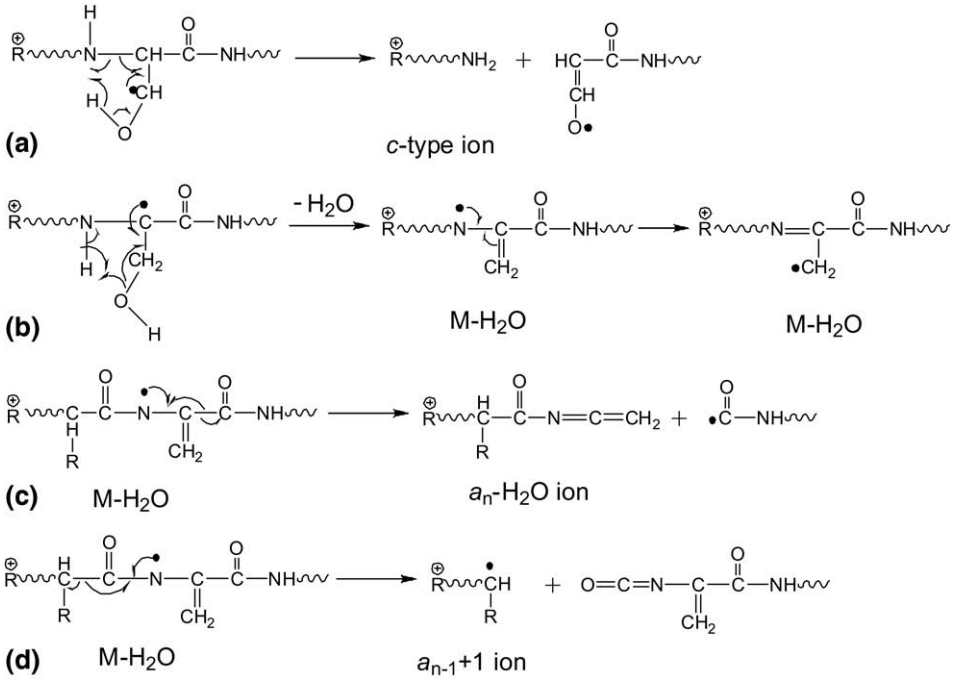

Scheme 4

4c and **d**. Cleavage of the C_α–C(O) bond to the right side yields an a_n-H_2O ion while cleavage of the C_α–C(O) bond on the left leads to an a_{n-1} + 1 ion. These two elimination pathways are probably competitive. Most a_n-H_2O ions that we observe are low in abundance, suggesting that this process is energetically less favored than formation of a_{n-1} + 1 ions. This is presumably because the former also leads to a carbonyl radical that is less stable than the α-radical shown in Scheme **4** [50, 53].

Charge-Driven Fragmentation

Although collisional activation of radical ions yields primarily *a*-type ions and side-chain losses, we occasionally observe a few *b*- and *y*- type fragments (referred as thermal fragments) that usually result from even-electron peptide ions upon vibrational excitation. To further investigate formation of these thermal fragments, radical ions containing proline were chosen since the Xxx-Pro bond easily cleaves during low-energy CID [29]. Figure S2-A displays the CID spectrum of a_7 + 1 radical ions generated by photodissociation of peptide ion RPPGFSP. Only certain *a*-, *y*-, and *c*-type ions appear. The a_5 ion is the most abundant fragment since it is formed at aromatic amino acid phenylalanine. a_5 + 1, c_5, and a_6 are induced by serine. In addition to these radical-induced fragment ions, two thermal fragments y_5 and y_6 ions are also observed. For comparison, the even-electron a_7 + 2 ion was also collisionally dissociated since the a_7 was low in abundance. The a_7 + 2 ion has the same structure as the a_7 + 1 ion except that the radical is replaced by a hydrogen atom. Its CID spectrum (Figure S2-B) contains primarily *y*-, *a*-, and *b*-type ions along with several internal fragment ions. The most abundant fragment is the y_6 ion corresponding to cleavage of the Arg–Pro bond and the y_5 ion is also evident. This suggests that y_5 and y_6 ions may be formed by charge-driven fragmentation processes even from a radical precursor. This is consistent with previous results from O'Hair and coworkers. In their experiments, collisional excitation of a variety of small glycine-containing peptide radical ions also leads to thermal fragments including b_n, b_n-H, and y_n ions [45]. They also demonstrated that radical fragmentation can be restricted to radical-driven processes when radical ions contain a fixed-charge group [54]. Charge-driven fragmentations have also been observed in other literatures of radical ion fragmentation [13, 14, 16, 43]. It is noteworthy that although the proton is initially sequestered on N-terminal arginine, C-terminal *y*-type ions are formed as shown in Figure S2-A and B. This is reasonable since vibrational activation mobilizes the ionizing proton on the N-terminal arginine. After peptide bond cleavage, *y*-type ions are formed when the proton moves to the C-terminal fragment.

Kinetic Competition Between Radical Transfer and Charge-Driven Fragmentation

To explore the rate that the unpaired electron can move following collisional activation, we have dissociated a series of homologous radical ions $[RAAADP(A)_{0-3}]^{+\bullet}$ (Figure S3 A–D). These ions contain a labile Asp–Pro bond that is easily cleaved upon collisional activation [55]. They also have similar structures except that the unpaired electron is different distances from aspartic acid. Asp–Pro cleavage and radical-induced cleavages following unpaired electron transfer are competitive processes. The resulting fragment intensities should depend on the initial radical location. The spectra in Figure S3 are similar in that they are all dominated by a_5, b_5, and b_5-H ions along with a neutral loss of 44 Da from aspartic side chain. The a_5 ion corresponds to backbone fragmentation at aspartic acid. The b_5 ion is formed via the cleavage of the Asp–Pro peptide bond [31]. As discussed previously, the b_5-H ion is also formed via cleavage of the Asp–Pro bond that proceeds after the hydrogen abstraction. The b_5-H/b_5 intensity ratio provides an indication of how fast the radical transfers from the C-terminus to aspartic acid. Expanded views of the b_5-H and b_5 ions are displayed in Figure 6a–d. The b_5/b_5-H ratio is plotted as open square points in Figure 6e as a function of the distance of the radical from the aspartic acid. It is evident that this ratio increases with this distance. When the radical is located on the adjacent proline, only b_5-H ions are formed. This indicates that the rate of radical transfer depends on the distance that the radical travels: the rate is higher when the distance is shorter. It appears to be comparable to or faster than the rate of charge-driven cleavage of the Asp–Pro peptide bond. The distance dependence implies that the radical transfer from the C-terminus to the aspartic acid is stepwise along the peptide backbone; otherwise, the four radicals would transfer at similar rates. This picture is consistent with what is known about radical migration during ECD. In that case, the unpaired electron in an α-radical transfers stepwise to various other α-carbons, inducing a "radical cascade" of backbone fragmentations [33, 36]. However, one cannot rule out the possibility that there is a similar distance dependence to the rate that radical ions fold.

Are Backbone Amide Hydrogens Transferable?

Although O'Connor and coworkers have demonstrated that backbone α-hydrogens can be easily abstracted [36], it is still unclear whether backbone amide-hydrogens are involved in the radical migration process. To address this issue, amide-hydrogens were replaced with deuterium by H/D exchange. CID spectra of deuterated radical ions $[RAAADP(A)_{0-2}]^{+\bullet}$ are displayed in Figures S4 A-C. These spectra appear similar to those from hydrogenated radical ions in Figure S3. The expanded views of b_5 fragment peaks are

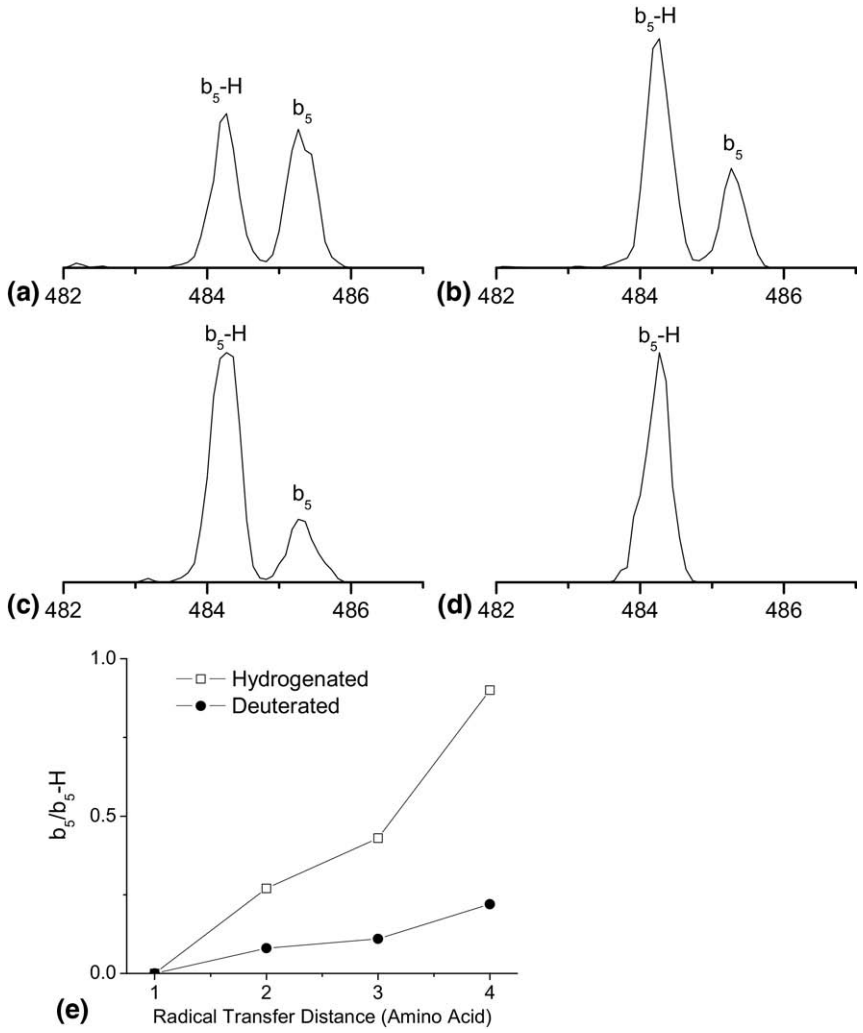

Figure 6. Expanded views of b_5 ions in the CID spectra of (**a**) a_9 + 1 and (**b**) a_8 + 1, (**c**) a_7 + 1, and (**d**) a_6 + 1 ions from peptide RAAADPAAAA (**e**) the b_5/b_5-H intensity ratio as a function of the radical transfer distance.

displayed in Figure S4-D. In all three spectra, only hydrogen-abstracted b_5-H ions are observed. Deuteron-abstracted b_5-D ions are at the level of noise. This suggests that backbone amide-hydrogens are probably not involved in the radical migration process; otherwise, both b_5-H and b_5-D ions would be formed. This is reasonable since nitrogen-centered radicals are much less stable than α-carbon centered radicals according to theoretical calculations [50]. The b_5/b_5-H ratio is plotted as solid circle points in Figure 6e as a function of the distance of the radical from the aspartic acid. It is evident that the b_5/b_5-H ratios in the deuterated spectra are much smaller than those in the hydrogenated spectra. This indicates that the rate of radical transfer is less affected by deuteration than the rate of Asp–Pro peptide bond cleavage. It is expected that cleavage of the Asp–Pro peptide bond becomes slower when the carboxylic acid is deuterated since it is facilitated by nucleophilic attack involving the aspartic side-chain [55].

Conclusion

We have demonstrated that 157 nm photodissociation of peptide ions with N-terminal arginine yields abundant a+1 radical ions. The radical in these odd-electron species has been shown to be located on the terminal α-carbon based on a-type ion formation at glycine and proline. Collisional activation of these radical ions yields abundant a-type ions at aromatic amino acids and side-chain losses at non aromatic amino acids. When aromatic amino acids are not present in the sequence, abundant a-type ions are observed at some nonaromatic amino acids. Serine and threonine induce unique fragmentation. In addition to a-type ions, they also lead to abundant c_{n-1} and a_{n-1} + 1 where n denotes the serine or threonine position. All of these fragmentation processes are directed by the movement of the radical from the terminal α-carbon to other amino acids following collisional activation. Competition among different fragmentation channels depends on the rela-

tive stabilities of the radical intermediates. In addition, thermal *b*- and *y*- type fragments are occasionally formed following cleavage of labile peptide bonds while hydrogen-deficient b_n-H ions are formed via hydrogen abstraction from regular *b*-type ions. Depending on the radical's initial location, the radical transfer process and the charge-driven fragmentation of labile Asp–Pro bonds can proceed at similar rates. The rate of radical transfer depends on the distance that the unpaired electron travels, implying that this process proceeds stepwise along the peptide sequence. The radical transfer process apparently does not involve amide-hydrogens.

Acknowledgments

The authors acknowledge support for this work by NSF grants CHE-0518234 and CHE-0431991.

Appendix A
Supplementary Material

Supplementary material associated with this article may be found in the online version at doi:10.1016/j.jasms.2009.03.02.

References

1. Halliwell, B.; Gutteridge, J. M. C. Free Radicals in Biology and Medicine; Oxford University Press: Oxford, 1999.
2. Pogozelski, W. K.; Tullius, T. D. Oxidative Strand Scission of Nucleic Acids: Routes Initiated by Hydrogen Abstraction from the Sugar Moiety. *Chem. Rev.* **1998,** *98*, 1089–1107.
3. Stubbe, J.; van der Donk, W. A. Protein Radicals in Enzyme Catalysis. *Chem. Rev.* **1998,** *98*, 705–762.
4. Garrison, W. M. Reaction-Mechanisms in the Radiolysis of Peptides, Polypeptides, and Proteins. *Chem. Rev.* **1987,** *87*, 381–389.
5. Dean, R. T.; Fu, S.; Stocker, R.; Davies, M. J. Biochemistry and Pathology of Radical-mediated Protein Oxidation. *Biochem. J.* **1997,** *324*, 1–18.
6. Hawkins, C. L.; Davies, M. J. Generation and Propagation of Radical Reactions on Proteins. *Biochim. Biophys. Acta* **2001**, *1504*, 196–219.
7. Rauk, A.; Yu, D.; Armstrong, D. A. Toward Site Specificity of Oxidative Damage in Proteins: C–H and C–C Bond Dissociation Energies and Reduction Potentials of the Radicals of Alanine, Serine, and Threonine Residues—An Ab Initio Study. *J. Am. Chem. Soc.* **1997,** *119*, 208–217.
8. Rauk, A.; Yu, D.; Armstrong, D. A. Oxidative Damage to and by Cysteine in Proteins: An Ab Initio Study of the Radicals Structures, C–H, S–H, and by Thiyl Radicals. *J. Am. Chem. Soc.* **1998,** *120*, 9949–8855.
9. Turecek, F.; Syrstad, E. A. Mechanism and Energetics of Intramolecular Hydrogen Transfer in Amide and Peptide Radicals and Cation Radicals. *J. Am. Soc. Chem.* **2003,** *125*, 3353–3369.
10. Chowdhury, S. K.; Katta, V.; Chait, B. T. Probing Conformational Changes in Proteins by Mass Spectrometry. *J. Am. Chem. Soc.* **1990,** *112*, 9012–9013.
11. Syka, J. E. P.; Coon, J. J.; Schroeder, M. J.; Shabanowitz, J.; Hunt, D. F. Peptide and Protein Sequence Analysis by Electron Transfer Dissociation Mass Spectrometry. *Proc. Natl. Acad. Sci. U.S.A.* **2004,** *101*, 9528–9533.
12. Zubarev, R. A.; Kelleher, N. L.; McLafferty, F. W. Electron Capture Dissociation of Multiply Charged Protein Cations. A Nonergodic Process. *J. Am. Soc. Chem.* **1998,** *120*, 3265–3266.
13. Chu, I. K.; Rodriquez, C. F.; Lau, T. C.; Hopkinson, A. C.; Siu, K. W. M. Molecular Radical Cations of Oligopeptides. *J. Phys. Chem. B* **2000,** *104*, 3393–3397.
14. Wee, S.; O'Hair, R. A. J.; McFadyen, W. D. Comparing the Gas-phase Fragmentation Reactions of Protonated and Radical Cations of the Tripeptides GXR. *Int. J. Mass Spectrom.* **2004,** *234*, 101–122.
15. Laskin, J.; Yang, Z.; Chu, I. K. Energetics and Dynamics of Electron Transfer and Proton Transfer in Dissociation of Metal III(Salen)–Peptide Complexes in the Gas Phase. *J. Am. Soc. Chem.* **2008,** *130*, 3218–3230.
16. Laskin, J.; Yang, Z.; Lam, C.; Chu, I. K. Charge-Remote Fragmentation of Odd-Electron Peptide Ions. *Anal. Chem.* **2007,** *79*, 6607–6614.
17. Hao, G.; Gross, S. S. Electrospray Tandem Mass Spectrometer Analysis of S- and N-Nitrosopeptides: Facile Loss of NO and Radical-Induced Fragmentation. *J. Am. Soc. Mass Spectrom.* **2006,** *17*, 1725–1730.
18. Hodyss, R.; Cox, H. A.; Beauchamp, J. L. Bioconjugates for Tunable Peptide Fragmentation: Free Radical Initiated Peptide Sequencing (FRIPS). *J. Am. Chem. Soc.* **2005,** *127*, 12436–12437.
19. Yin, H.; Chacon, A.; Porter, N. A.; Yin, H.; Masterson, D. S. Free Radical-Induced Site-Specific Peptide Cleavage in the Gas Phase: Low-Energy Collision-Induced Dissociation in ESI- and MALDI Mass Spectrometry. *J. Am. Soc. Mass Spectrom.* **2007,** *18*, 807–816.
20. Ly, T.; Julian, R. R. Residue-Specific Radical-Directed Dissociation of Whole Proteins in the Gas Phase. *J. Am. Soc. Chem.* **2008,** *130*, 351–358.
21. Oh, H. B.; Breuker, K.; Sze, S. K.; Ge, Y.; Carpenter, B. K.; McLafferty, F. W. Secondary and Tertiary Structures of Gaseous Protein Ions Characterized by Electron Capture Dissociation Mass Spectrometry and Photofragment Spectroscopy. *Proc. Natl. Acad. Sci. U.S.A.* **2002,** *99*, 15863–15868.
22. Breuker, K.; Oh, H. B.; Horn, D. M.; Cerda, B. A.; McLafferty, F. W. Detailed Unfolding and Folding of Gaseous Ubiquitin Ions Characterized by Electron Capture Dissociation. *J. Am. Soc. Chem.* **2002,** *127*, 6407–6420.
23. Swaney, D. L.; McAlister, G. C.; Wirtala, M.; Schwartz, J. C.; Syka, J. E. P.; Coon, J. J. Supplemental Activation Method for High-Efficiency Electron-Transfer Dissociation of Doubly Protonated Peptide Precursors. *Anal. Chem.* **2007,** *79*, 477–485.
24. Barlow, C. K.; McFadyen, W. D.; O'Hair, R. A. J. Formation of Cationic Peptide Radicals by Gas-Phase Redox Reactions with Trivalent Chromium, Manganese, Iron, and Cobalt Complexes. *J. Am. Soc. Chem.* **2005,** *127*, 6109–6115.
25. Sun, Q.; Nelson, H.; Ly, T.; Stoltz, B. M.; Julian, R. R. Side Chain Chemistry Mediates Backbone Fragmentation in Hydrogen Deficient Peptide Radicals. *J. Proteome Res.* **2008,** *8*, 958–966.
26. Ly, T.; Julian, R. R. Tracking Radical Migration in Large Hydrogen Deficient Peptides with Covalent Labels: Facile Movement Does Not Equal Indiscriminate Fragmentation. *J. Am. Soc. Mass Spectrom.* **2009,** *In press*.
27. Burlet, O.; Orkiszewski, R. S.; Ballard, K. D.; Gaskell, S. J. Charge Promotion of Low-energy Fragmentation of Peptide ions. *Rapid Commun. Mass Spectrom.* **1992,** *6*, 658–662.
28. Dongre, A. R.; Jones, J. L.; Somogyi, A.; Wysocki, V. H. Influence of Peptide Composition, Gas-Phase Basicity, and Chemical Modification on Fragmentation Efficiency: Evidence for the Mobile Proton Model. *J. Am. Soc. Chem.* **1996,** *118*, 8365–8374.
29. Kapp, E. A.; Schutz, F.; Reid, G. E.; Eddes, J. S.; Moritz, R. L.; O'Hair, R. A. J.; Speed, T. P.; Simpson, R. J. Mining a Tandem Mass Spectrometry Database to Determine the Trends and Global Factors Influencing Peptide Fragmentation. *Anal. Chem.* **2003,** *75*, 6251–6264.
30. Paizs, B.; Suhai, S. Towards Understanding the Tandem Mass spectra of Protonated Oligopeptides. 1: Mechanism of Amide Bond Cleavage *J. Am. Soc. Mass Spectrom.* **2004,** *15*, 103–113.
31. Wysocki, V. H.; Tsaprailis, G.; Smith, L. L.; Breci, L. A. Mobile and Localized Protons: A Framework for Understanding Peptide Dissociation. *J. Mass Spectrom.* **2000,** *35*, 1399–1406.
32. Cooper, H. J.; Hudgins, R. R.; Hakansson, K.; Marshall, A. G. Characterization of Amino Acid Side-Chain Losses in Electron Capture Dissociation. *J. Am. Soc. Mass Spectrom.* **2002,** *13*, 241–249.
33. Leymarie, N.; Costello, C. E.; O'Connor, P. B. Electron Capture Dissociation Initiates a Free Radical Reaction Cascade. *J. Am. Chem. Soc.* **2003,** *125*, 8949–8958.
34. Fung, Y. M. E.; Chan, T. W. D. Experimental and Theoretical Investigations of the Loss of Amino Acid Side Chains in Electron Capture Dissociation of Model Peptides. *J. Am. Soc. Mass Spectrom.* **2005,** *16*, 1523–1535.
35. Zubarev, R. A.; Kruger, N. A.; Fridriksson, E. K.; Lewis, M. A.; Horn, D. M.; Carpenter, B. K.; McLafferty, F. W. Electron Capture Dissociation of Gaseous Multiply-Charged Proteins Is Favored at Disulfide Bonds and Other Sites of High Hydrogen Atom Affinity. *J. Am. Chem. Soc.* **1999,** *121*, 2857–2862.
36. O'Connor, P. B.; Lin, C.; Cournoyer, J. J.; Pittman, J. L.; Belyayev, M.; Budnik, B. A. Long-Lived Electron Capture Dissociation Product Ions Experience Radical Migration via Hydrogen Abstraction. *J. Am. Soc. Mass Spectrom.* **2006,** *17*, 576–585.
37. Han, H.; Xia, Y.; McLuckey, S. A. Ion Trap Collisional Activation of c and z Ions Formed via Gas-Phase Ion/Ion Electron-Transfer Dissociation. *J. Proteome Res.* **2007,** *6*, 3062–3069.
38. Cui, W.; Thompson, M. S.; Reilly, J. P. Pathways of Peptide Ion Fragmentation Induced by Vacuum Ultraviolet Light. *J. Am. Soc. Mass Spectrom.* **2005,** *16*, 1384–1398.
39. Zhang, L.; Cui, W.; Thompson, M. S.; Reilly, J. P. Structures of *a*-Type Ions Formed in the 157 nm Photodissociation of Singly-Charged Peptide Ions. *J. Am. Soc. Mass Spectrom.* **2006,** *17*, 1315–1321.
40. Thompson, M. S.; Cui, W.; Reilly, J. P. Fragmentation of Singly Charged Peptide Ions by Photodissociation at $\lambda = 157$ nm. *Angew. Chem. Int. Edit.* **2004,** *43*, 4791–4794.
41. Kim, T. Y.; Thompson, M. S.; Reilly, J. P. Peptide Photodissociation at 157 nm in a Linear Ion Trap Mass Spectrometer. *Rapid Commun. Mass Spectrom.* **2005,** *19*, 1657–1665.
42. Chu, I. K.; Zhao, J.; Xu, M.; Siu, S. O.; Hopkinson, A. C.; Siu, K. W. M. Are the Radical Centers in Peptide Radical Cations Mobile? The Generation, Tautomerism, and Dissociation of Isomeric α-Carbon-

Centered Triglycine Radical Cations in the Gas Phase. *J. Am. Soc. Chem.* **2008,** *130*, 7862–7872.
43. Chu, I. K.; Rodriguez, C. F.; Hopkinson, A. C.; Siu, K. W. M.; Lau, T. C. Formation of Molecular Radical Cations of Enkephalin Derivatives Via Collisional-Induced Dissociation of Electrospray-generated Copper (II) Complex Ions of Amines and Peptides. *J. Am. Soc. Mass Spectrom.* **2001,** *12*, 1114–1119.
44. Hopkinson, A. C.; Siu, K. W. M. In *Principles of Mass Spectrometry Applied to Biomolecules*; Laskin, J.; Lifshitz, C., Eds.; Wiely-Interscience: Hoboken, NJ, 2006; p 301–335.
45. Wee, S.; O'Hair, R. A. J.; McFadyen, W. D. The Role of the Position of the Basic Residue in the Generation and Fragmentation of Peptide Radical Ions. *Int. J. Mass Spectrom.* **2006,** *249*, 171–183.
46. Moran, D.; Jacob, R.; Wood, G. P. F.; Coote, M. L.; Davies, M. J.; O'Hair, R. A. J.; Easton, C. J.; Radom, L. Rearrangements in Model Peptide-Type Radicals Via Intramolecular Hydrogen-Atom Transfer. *Helv. Chim. Acta* **2006,** *89*, 2254–2272.
47. Wee, S.; O'Hare, R. A. J.; McFadyen, W. D. Side-Chain Radical Losses from Radical Cations Allows Distinction of Leucine and Isoleucine Residues in the Isomeric Peptide Gly-XXX-Arg. *Rapid Commun. Mass Spectrom.* **2002,** *16*, 884–890.
48. Peter, M. G. Chemical Modifications of Biopolymers by Quinones and Quinone Methides. *Angew. Chem. Int. Edit.* **1989,** *28*, 555–570.
49. Kjeldsen, F.; Haselmann, K. F.; Sorensen, E. S.; Zubarev, R. A. Distinguishing of Ile/Leu Amino Acid Residues in the PP3 Protein by (Hot) Electron Capture Dissociation in Fourier Transform Ion Cyclotron Resonance Mass Spectrometry. *Anal. Chem.* **2003,** *75*, 1267–1274.
50. Wood, G. P. F.; Moran, D.; Jacob, R.; Radom, L. Bond Dissociation Energetics and Radical Stabilization Energies Associated with Model Peptide-Backbone Radicals. *J. Phys. Chem. A* **2005,** *109*, 6318–6325.
51. Wood, G. P. F.; Easton, C. J.; Rauk, A.; Davies, M. J.; Radom, L. Effect of Side Chains on Competing Pathways for β-Scission Reactions of Peptide-Backbone Alkoxyl Radicals. *J. Phys. Chem. A* **2006,** *110*, 10316–10323.
52. Smith, L. L.; Herrmann, K. A.; Wysocki, V. H. Investigation of Gas Phase Ion Structure for Proline-Containing b_2 Ion. *J. Am. Soc. Mass Spectrom.* **2006,** *17*, 20–28.
53. Wood, G. P. F.; Easton, C. J.; Rauk, A.; Davies, M. J.; Radom, L. Effect of Side Chains on Competing Pathways for β-Scission Reactions of Peptide-Backbone Alkoxyl Radicals. *J. Phys. Chem. A* **2008,** *110*, 10316–10323.
54. Karnezis, A.; Barlow, C. K.; O'Hair, R. A. J.; McFadyen, W. D. Peptide Derivatization as a Strategy to Form Fixed-Charge Peptide Radicals. *Rapid Commun. Mass Spectrom.* **2006,** *20*, 2865–2870.
55. Tsaprailis, G.; Somogyi, A.; Nikolaev, E. N.; Wysocki, V. H. Refining the Model for Selective Cleavage at Acidic Residues in Arginine-Containing Protonated Peptides. *Int. J. Mass Spectrom.* **2000**, *195/196*, 467–479.